ELSEVIER

Journal of Microbiological Methods 40 (2000) 89–97

Journal of Microbiological Methods

www.elsevier.com/locate/jmicmeth

Quantification of bacterial adhesion forces using atomic force microscopy (AFM)

Herbert H.P. Fang[a,*], Kwong-Yu Chan[b], Li-Chong Xu[a]

[a]*Centre for Environmental Engineering Research, Department of Civil Engineering, The University of Hong Kong, Pokfulam Road, Hong Kong*

[b]*Department of Chemistry, The University of Hong Kong, Pokfulam Road, Hong Kong*

Received 22 July 1999; received in revised form 22 November 1999; accepted 22 November 1999

Abstract

This study demonstrated that atomic force microscopy (AFM) can be used to obtain high-resolution topographical images of bacteria, and to quantify the tip–cell interaction force and the surface elasticity. Results show that the adhesion force between the Si_3N_4 tip and the bacteria surface was in the range from -3.9 to -4.3 nN. On the other hand, the adhesion forces at the periphery of the cell–substratum contact surface ranged from -5.1 to -5.9 nN and those at the cell–cell interface ranged from -6.5 to -6.8 nN. The two latter forces were considerably greater than the former one, most likely due to the accumulation of extracellular polymer substance (EPS). Results also show that the elasticity varied on the cell surface.

Keywords: Adhesion force; Atomic force microscopy (AFM); Bacteria; Cell; Elasticity; Extracellular polymer substance (EPS)

1. Introduction

Bacterial adhesion to a solid surface is a crucial step in the process of biofilm formation. It is a subject which has attracted much investigating by microbiologists, physical chemists, materials scientists, and civil engineers (Jucker et al., 1998). As bacteria move toward a solid surface, the initial interaction between the cell and the surface is governed by long and medium range forces, primarily van der Waals and electrostatic forces (Fletcher, 1996; Razatos et al., 1998). These forces depend on the physicochemical properties of substratum and the bacterial surface, such as hydrophobicity (Gannon et al., 1991), free energy (Busscher et al., 1984), and surface charge (Gannon et al., 1991). Busscher et al. (1998) have analyzed and compared the magnitudes of lateral and perpendicular interaction forces involved in mobile and immobile adhesion of cells on solid surfaces. Extracellular polymeric substance (EPS) secreted by the bacteria and the bacterial flagella also play an important role in the adhesion and subsequent biofilm formation.

The traditional method of evaluating the adhesive propensity of bacteria is by enumeration of bacteria attached to the surface through microscopic image analyses (Caldwell and Germida, 1985; Evans-Hurrell et al., 1993; An and Friedman, 1997). Electron

*Corresponding author. Tel: +852-2859-2660; fax: +852-2559-5337.

E-mail address: hrechef@hkucc.hku.hk (H.H.P. Fang)

0167-7012/00/$ – see front matter
PII: S0167-7012(99)00137-2

microscopy (Knutton, 1995) and confocal laser scanning microscopy (Manning, 1995) have been used for this purpose. The adhesion strength of biofilm, on the other hand, could be estimated from the intensity of increased tensile and shear forces at the levels where biofilm begins to peel off (Ohashi and Harada, 1996). However, all of these methods are imprecise, indirect and time consuming. The latest development in atomic force microscopy offers new opportunities in characterizing the bacterial surface. Utilizing a microprobe (tip) mounted on a flexible cantilever scanning across the surface, the AFM can obtain topographical images of the cell surface at molecular resolution (Lal and John, 1994; Teiko et al., 1994; Hansma et al., 1997). In addition, it is also a powerful tool for investigating nanometric physicochemical and mechanical properties of cell surface (Fritz et al., 1994; Hoh and Schoenenberger, 1994). A force–distance curve records the variations of interaction forces as the cell sample approaches the tip, makes contact and then retrieves from the tip. Such a force–distance curve provides valuable information on the tip–cell interaction, which is sensitive to the chemical nature of both the tip and the cell surface (Lyubchenko et al., 1993; Van der Werf et al., 1994).

This study was conducted to quantify the AFM tip–cell interaction forces over the various sections of a bacterial cell surface and at various interfacial regions after the preliminary formation of a biofilm. From the slope of the repulsive section of a force–distance curve, the cell surface elasticity can be measured. This information may lead to a better understanding of the formation mechanism of biofilm.

2. Materials and methods

2.1. Bacteria and growth condition

Sulfate-reducing bacteria (SRB) were chosen for this study. This group of bacteria is known to be responsible for the microbial fouling on various surfaces, ranging from ship hulls to heat exchangers and wastewater pipelines. SRB were first enriched and isolated from marine sediments of the Victoria Harbour, Hong Kong. The isolated SRB was then cultured at 30°C in seawater using a modified Postgate's medium C (Videla, 1996). The seawater was sterilized by filtering through a 0.45 μm membrane before use. Each liter of seawater medium contained 0.5 g KH_2PO_4; 1 g NH_4Cl; 0.06 g $CaCl_2 6H_2O$; 0.06 g $MgSO_4 7H_2O$; 6 ml sodium lactate (70%); 1 g yeast extract; 0.004 g $FeSO_4 7H_2O$; 0.3 g sodium citrate and 2200 mg of sulfate. The pH was adjusted to 7.2 ± 0.1 using 1 M NaOH solution.

2.2. Bacteria and biofilm preparation and AFM operation

The experimental procedure for biofilm preparation was similar to that described in a previous study of biofilm induced mild steel corrosion (Xu et al., in press). In this study, mica was chosen instead as a substratum for the bacteria attachment and the formation of biofilm. Immediately after cleavage in the clean atmosphere, mica specimens were mounted to steel discs and immersed in the seawater medium containing SRB. Bacterial cells began to attach to the mica sheets after having been immersed in the SRB containing seawater during hours 1–4. Developing biofilms can be observed after 8 h. Specimens were taken out from the seawater after different periods of immersion, lightly rinsed in sterile distilled water and then dried in a desiccator over night before AFM examination. A Nanoscope IIIA AFM (Digital Instruments, Santa Barbara, CA, USA) operating in contact mode in air was used to image cells and to measure interaction forces. The relative humidity was 50–60% and no capillary forces were observed during the AFM operation. The nanoprobe cantilevers were made of silicon nitride (Si_3N_4) with a spring constant of $k = 0.06$ N/m (Digital Instruments). The radius of curvature of the AFM tip is approximately 50 nm. The Digital Nanoscope software (version 4.23) was used to analyze the topographic images of the surface, as well as the force–distance over the sample surface. During the force–distance measurements, the scanning rate in *z*-direction was maintained at 30 Hz. Each map of sample surface consisted of 64×64 grid points. Only the vertical adhesion forces between the AFM tip and the cell surface were measured; lateral interaction forces were not investigated in this study.

3. Results and discussion

3.1. Images of bacteria and biofilm on mica

Fig. 1a illustrates the typical image of isolated SRB cells attached on the mica surface after immersing in seawater for 4 h. As cells multiplied in the nutrient-rich seawater medium, they aggregated to form clusters as illustrated in Fig. 1b, the image of which was taken after 8 h. The bacterial morphology

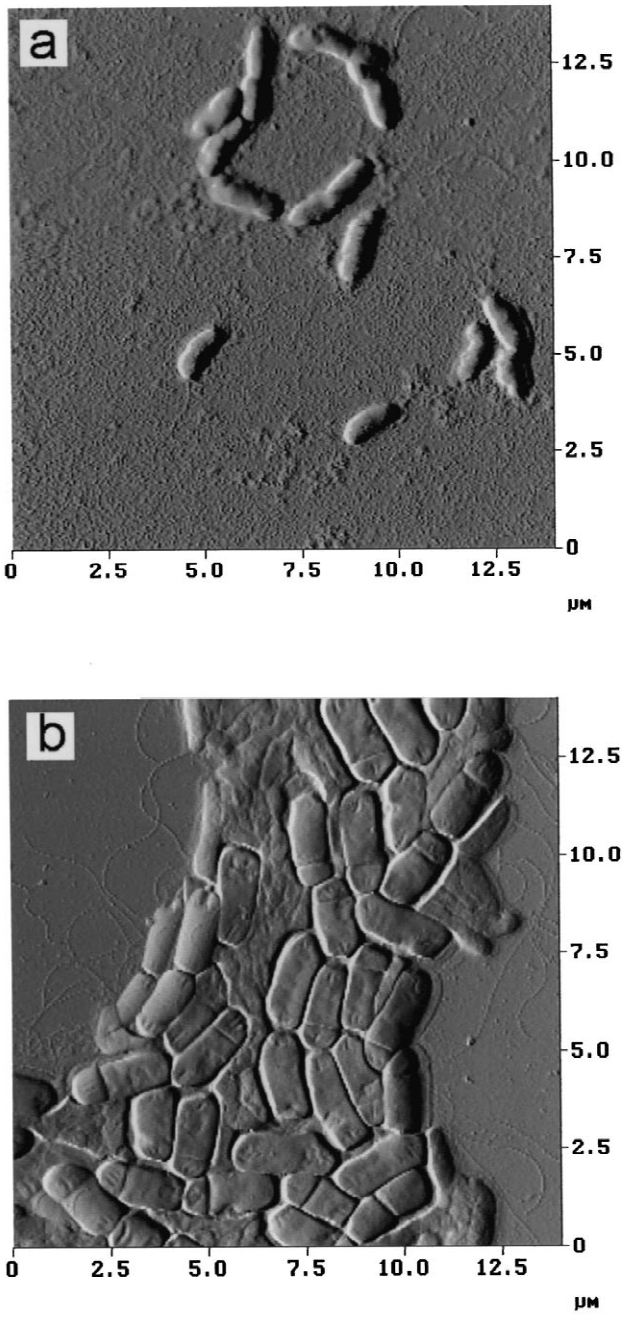

Fig. 1. Contact mode AFM images of a mica surface with (a) scattered SRB cells and (b) clustered SRB cells.

and flagella are clearly visible. Biofilms covering the whole coupon surface were observed thereafter. As compared to scanning electron micrographs (SEM), AFM images in Figs. 1a and 1b are superior in resolution and definition in the vertical dimension. In addition, to prepare for AFM imaging, the cell surface needs not be placed under vacuum and sputtered with conductive gold or carbon, as required in SEM.

AFM measurements were conducted at 20°C in dry air (50–60% relative humidity) to avoid the influence of capillary condensation of water (Binggeli and Mate, 1994). Capillary forces between the AFM tip and a wet surface could interfere with the imaging and force measurement. These capillary forces can be avoided by operating the AFM with tip and substratum completely immersed in solution. This also allows in-situ imaging of dynamic surfaces. However, resolutions of image and force curves could be reduced due to fluctuations of solvation forces. Conducting the AFM in air also avoids the attachment of suspended particulates and bacterial cells to the tip.

On the other hand, physiochemical changes to the cells may occur during the drying process. Pembrey et al. (1999) found that air drying affected some cell properties, such as affinity to Sepharose columns, attachment to solid substrata, and electrophoretic mobility of cells, but had little or no effect on hydrophobicity and viability. The effect of air drying on the adhesion forces was not investigated in this study. However, it was observed that for a given sample the images and force data obtained in air were stable and reproducible with repeated AFM operations. Thus, dehydration effects, if any, would probably occur only in the short period immediately after samples leaving solution.

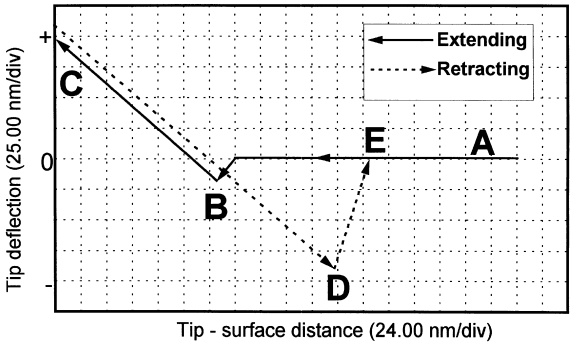

Fig. 2. A typical force–distance curve between the AFM tip and bacterium surface.

3.2. Determination of vertical tip–cell interaction force

Fig. 2 illustrates a typical force–distance curve between the Si_3N_4 tip and the cell surface. As the sample extends upward approaching the tip from A to B, the tip is pulled down by the attractive force and jump-to-contact with the surface at B. As the sample continues to extend, the cantilever bends upward as the tip presses onto the surface. When the tip reaches position C, the sample retracts from the tip and the cantilever relaxes. As the sample continues to retract, the cantilever begins to bend downward (CD) due to the adhesion force, until reaching the break point (D) at which the cantilever rebounds sharply upward to E. The adhesion force between tip and surface can be calculated from the deflection distance of cantilever and the cantilever spring constant, as follows:

$$F = k \times \Delta L$$

where F is force (nN), k is the spring constant of cantilever, which was equal to 0.06 N/m in this study, and ΔL is the deflection distance (nm), which in Fig. 2 is the vertical distance between points D and A. The reference zero of deflection is point A, when the tip is far away from the surface. A negative deflection corresponds to attractive force whereas a positive deflection corresponds to repulsive force.

The force–distance curve also provides additional information related to the elasticity of the sample surface. The cantilever deflection increases as the tip continues to press into the sample after contact, as represented by the repulsive section of the force curve BC in Fig. 2. The slope of the BC section of the force curve represents the surface elasticity (Radmacher et al., 1994).

3.3. Tip–cell interaction forces on bacteria surface and at cell–substratum periphery

Figs. 3a and 3b illustrate typical 3-D and 2-D topographic images of a bacterial cell adhered onto

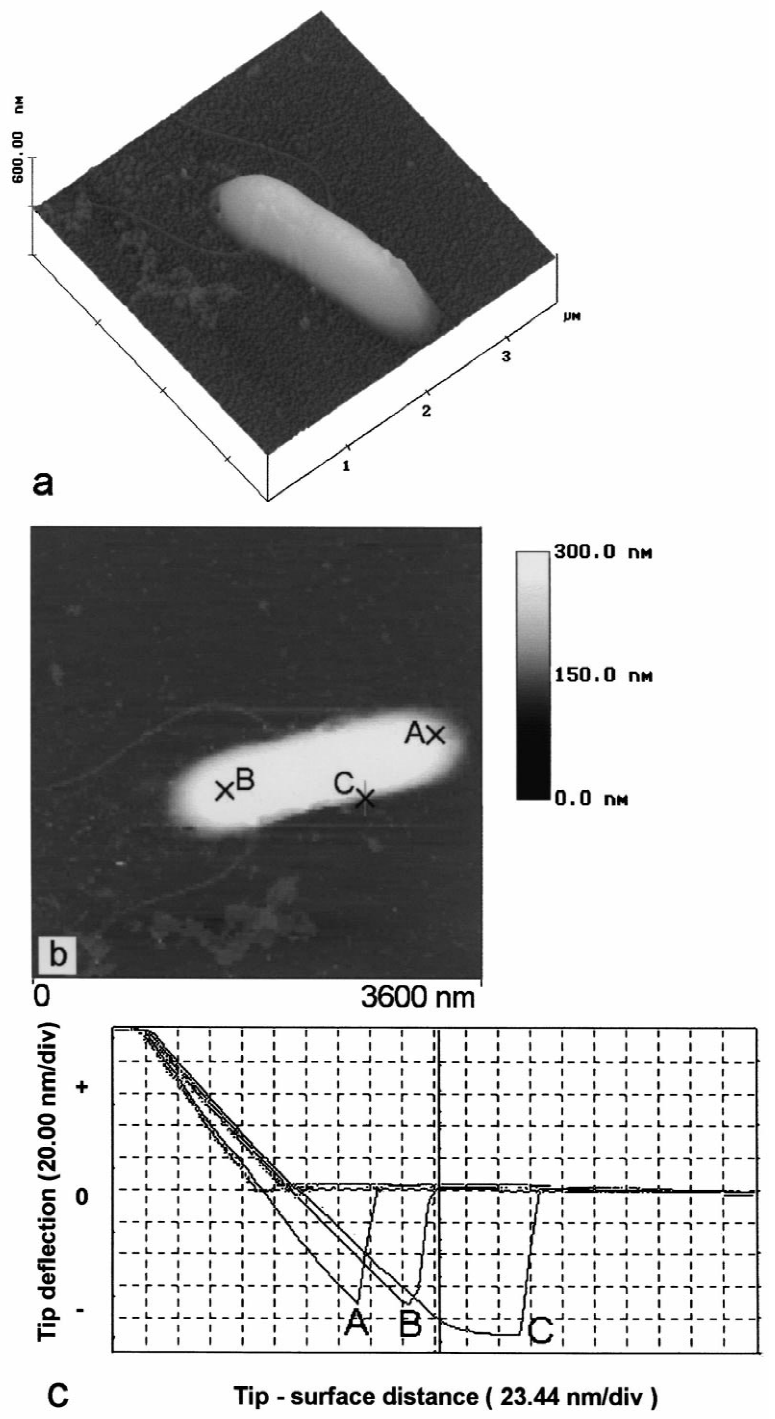

Fig. 3. Contact mode AFM images of a bacterial cell in (a) 3-D display, (b) 2-D display, and (c) the corresponding force curves at locations A, B, and C.

the mica surface after 1 h of immersion in seawater medium. The dimensions ($L \times W \times D$ for the cell were $2.37 \times 0.62 \times 0.23$ μm), shape and flagella of the bacteria are clearly visible. Fig. 3c is the force–distance curves at three selected locations of the cell surface A, B and C, as marked in Fig. 3b. Since the tip scanned over the two-dimensional grided cell surface, up to thousands of such curves could be obtained over the cell surfaces at various locations. What are shown in Fig. 3c represent only three of these curves.

In Fig. 3c, the maximum downward deflections during sample retraction were −68.0, −70.8 and −90.0 nm, respectively, at locations A, B and C. The corresponding forces at the respective locations are, thus, −4.08, −4.25 and −5.40 nN, as calculated from the spring constant of 0.06 N/m. This shows that the adhesion force at location C, which is at the periphery of the cell–substratum contact surface, is considerably higher than those at locations A and B, both of which are on the cell surface. Force–distance curves obtained at hundreds of grid point locations show similar results. The average force over the cell surface was −4.07 nN with a standard deviation of 0.40 nN. On the other hand, the average adhesion force at the cell–substratum periphery was -5.08 ± 0.40 nN.

The adhesion force at the cell–substratum periphery was 25% higher than those on the cell surface. This was most likely due to the accumulation of EPS at the cell–substratum periphery, considerably enhancing the bacteria binding to surface (Vandevevere and Kirchman, 1993; Fletcher, 1996). On the other hand, the adhesion force of flagella was -4.13 ± 0.23 nN, similar to that of the cell surface. The similarity in adhesion force is expected because there is no EPS on surface of flagella (Lawrence et al., 1987), the main function of which is to propel cells in solution until cells are attached to the solid surface.

The slopes of force–distance curves after the initial tip contact with the sample represent the elasticity of the cell surface. Fig. 3c illustrates that the elasticity varied on the cell sruface. The surface elasticities at two of cell surface locations A and B are quite different. The surface elasticity at location B was in fact nearly identical to that at the location C, which was at the cell–substratum periphery.

Rotsch and Radmacher (1997) found in an AFM study that the interaction forces between the tip and a charged surface were affected by the ionic strength of the solution. It is possible that the ionic strength may also affect the elasticity of the cell surface. However, this issue is beyond the scope of this study, and further investigation is warranted.

3.4. Tip–cell adhesion force on cell–cell interface of a developing biofilm

After initial attachment to the solid surface, cells began to cluster due to the binding force at the interface resulting from the increased accumulation of EPS. As the clustering process continues to proceed, cells gradually cover the complete solid surface forming a biofilm. In this study, cell attachment was observed within 1 h of immersing mica in the seawater medium. Cells clusters were observed within 4 h, and biofilms were formed in 8 h.

Fig. 4a gives the image of a developing SRB biofilm surface after 8 h of immersion. Individual bacterial cells are visible. Fig. 4b shows the corresponding force map of the biofilm. The gray scale of each pixel represents the intensity of the force at that location of the map. A bright spot indicates positive deflection (repulsive force) and a dark spot represents negative deflection (attractive force). Fig. 4c illustrates the force–distance curves at two locations A and B. The former location is on the cell surface and the latter at the cell–cell interface.

Fig. 4b shows that the forces were more attractive at the cell–cell interface than on the cell surface. The average force on cell surface in the 8-h biofilm was -4.10 ± 0.39 nN. This is nearly identical to those observed in Fig. 3 for individual cells after 1 h of immersion. The force at the cell–cell interface was -6.81 ± 0.53 nN, considerably more attractive than those observed for individual cells in Fig. 3. This seems to suggest that the accumulation of sticky EPS on cell–cell interface would enhance the aggregation of bacterial cells, leading to the formation of a spreading biofilm. The forces of the cell surface and the interface were measured for samples taken at six time intervals, from hour 1 to hour 36. Table 1 summarizes the adhesion force values of these samples. Results show that the force at bacterial cells surface changed little from −3.87 to −4.25 nN over

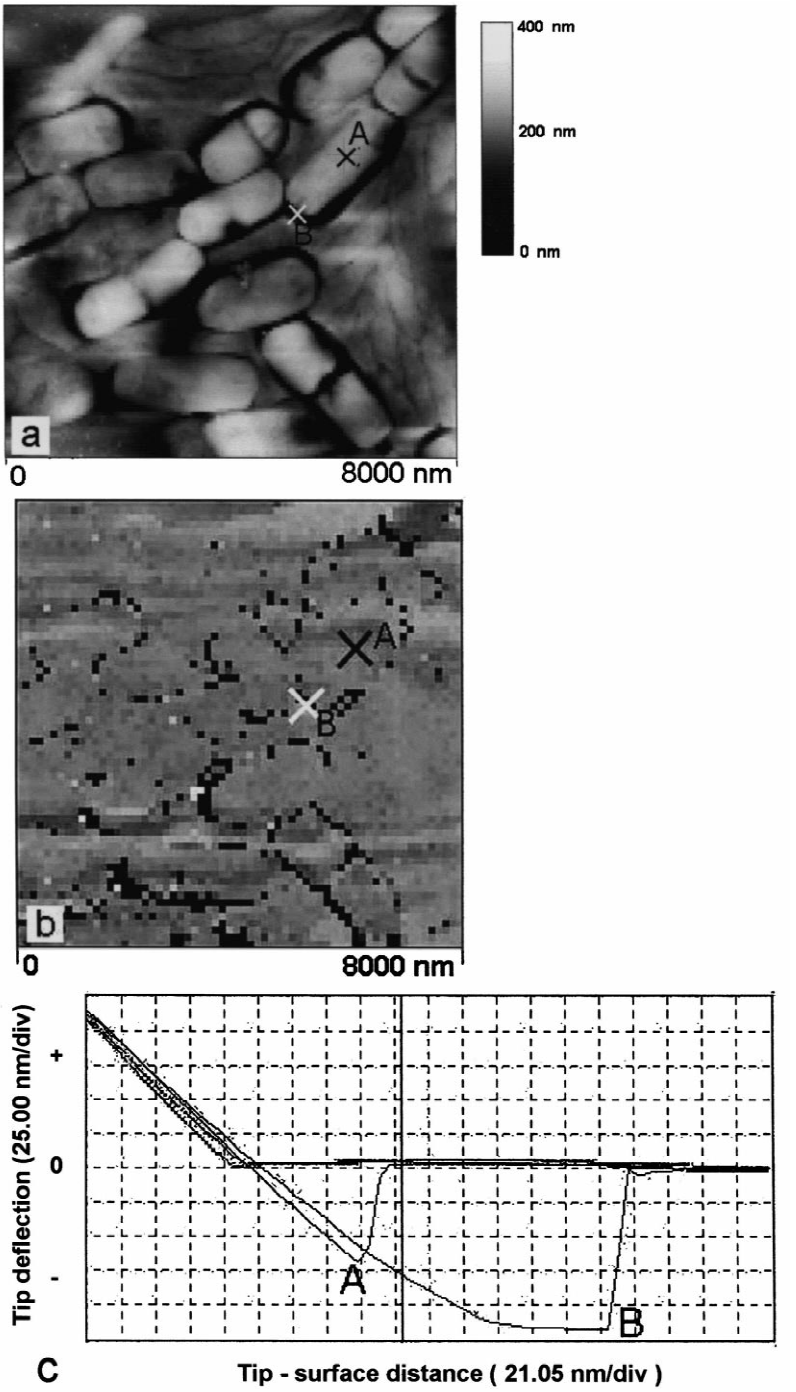

Fig. 4. (a) Contact mode AFM image of a developing biofilm, (b) the corresponding force distribution map, and (c) force curves at locations A and B.

Table 1
Tip–surface adhesion forces on cell surface, at cell–cell interface and at cell–substratum periphery (mean±S.D.)

Time (h)	Bacteria surface (nN)	Cell–substratum periphery (nN)	Cell–cell interface (nN)
1	−4.07±0.40	−5.08±0.40	n/a[a]
2	−4.08±0.47	−5.37±0.60	n/a
4	−4.25±0.39	−5.88±0.70	n/a
8	−4.10±0.31	n/a	−6.81±0.53
12	−3.87±0.74	n/a	−6.49±0.52
36	−3.96±0.39	n/a	−6.78±0.77

[a] n/a: not applicable.

a 36-h period, whereas those at the cell–substratum periphery changed from −5.08 nN at hour 1 to −5.88 nN at hour 4. After the formation of a biofilm (hour 8), the adhesion force at the cell–cell interfaces increased to a range from −6.50 to −6.80 nN.

The interfacial force between cell and substratum could not be probed directly by the present study. One would need to devise a method of stickying the AFM probe to the bacterium cell and measure the force required to lifting the cell from the substratum surface. However, in this study in the retracting scan of the AFM tip force curve measurement, no detachment of cells was ever observed. This seems to imply that the tip–cell force was not strong enough to overcome the cell–substratum interfacial force.

Theories accounting for van der Waals, electrostatic, and double-layer energies have been applied to cells mobility (Rutter and Vincent, 1988; Oshima and Kondo, 1991; Busscher et al., 1998). However, few experimental measurements were reported in the literature for the vertical force required to pull off an attached bacterium. The vertical adhesion forces measured in this study was in the order of 10 nN, which is typical for AFM measurements on many materials. Assuming a spherical interaction surface of the AFM tip with a radius of curvature of 50 nm, the adhesion forces in this study were in the order of 10^5 N/m^2. For comparison, the lateral shearing forces required to separate attached cells were reported in the range between 0.081 to 54 N/m^2 (Rutter and Vincent, 1988), several orders of magnitude lower than those observed in this study.

4. Conclusions

Atomic force microscopy is a powerful tool for studying the adhesion forces on a single bacterium cell surface, on cell–cell interface, and on the periphery of the cell–substratum contact surface. It provides high resolution topographic images as well as quantitative information about surface force and elasticity. This may lead to a better understanding of the biofilm formation mechanism. The force between the AFM tip and bacterial cell surface was at a relatively constant level of −3.9 to −4.3 nN. On the other hand, the adhesion forces at the cell–substratum periphery ranged from −5.1 to −5.9 nN and that at the cell–cell interface ranged from −6.5 to −6.8 nN. The higher adhesion forces were most likely due to the accumulation of extracellular polymer substance (EPS). Elasticity was found varying on the cell surface.

Acknowledgements

The authors would like to thank the financial support of this study by the Hong Kong Research Grants Council.

References

An, Y.H., Friedman, R.J., 1997. Laboratory methods for studies of bacterial adhesion. J. Microbiol. Methods 30, 141–152.

Binggeli, M., Mate, C.M., 1994. Influence of capillary condensation of water on nanotribology studied by force microscopy. Appl. Phys. Lett. 65, 415–417.

Busscher, H.J., Weerkamp, A.H., van der Mei, H.C., van Pelt, A.W.J., De Jong, H.P., Arends, J., 1984. Measurements of the surface free energy of bacterial cell surfaces and its relevance for adhesion. Appl. Environ. Microbiol. 48, 980–983.

Busscher, H.J., Poortinga, A.T., Bos, R., 1998. Lateral and perpendicular interaction forces involved in mobile and immobile adhesion of microorganisms on model solid surfaces. Curr. Microbiol. 37, 319–323.

Caldwell, D.E., Germida, J.J., 1985. Evaluation of difference imagery for visualizing and quantitating microbial growth. Can. J. Microbiol. 31, 35–44.

Evans-Hurrell, J.A., Adler, J., Denyer, S., Rogers, T.G., Williams, P., 1993. A method for the enumeration of bacterial adhesion to epithelial cells using images analysis. FEMS Microbiol. Lett. 107, 77–82.

Fletcher, M., 1996. Bacterial attachment in aquatic environments: a diversity of surfaces and adhesion strategies. In: Fletcher, M. (Ed.), Bacterial Adhesion: Molecular and Ecological Diversity, Wiley–Liss, New York, pp. 1–24.

Fritz, M., Radmacher, M., Gaub, H.E., 1994. Visualization and identification of intracellular structures by force modulation microscopy and drug induced degradation. J. Vac. Sci. Technol. B 12, 1526–1529.

Gannon, J.T., Manilal, V.B., Alexander, M., 1991. Relationship between cell surface properties and transport of bacteria through soil. Appl. Environ. Microbiol. 57, 190–193.

Hansma, H.G., Kim, K.J., Laney, D.E., Garcia, R.A., Argaman, M., Allen, M.J., Parsons, S.M., 1997. Properties of biomolecules measured from atomic force microscope images: a review. J. Struct. Biol. 119, 99–108.

Hoh, J.H., Schoenenberger, C.A., 1994. Surface morphology and mechanical properties of MDCK monolayers by atomic force microscopy. J. Cell Sci. 107, 1105–1114.

Jucker, B.A., Zehnder, A.J.B., Harms, H., 1998. Quantification of polymer interaction in bacterial adhesion. Environ. Sci. Technol. 32, 2909–2915.

Knutton, S., 1995. Electron microscopical methods in adhesion. In: Doyle, R.J., Ofek, I. (Eds.), Methods in Enzymology, Vol. 253, Academic Press, California, pp. 145–158.

Lal, R., John, S.A., 1994. Biological application of atomic force microscopy. Am. J. Physiol.: Cell Physiol. 266, C1–C21.

Lawrence, J.R., Delaquis, P.J., Korber, D.R., Caldwell, D.E., 1987. Behavior of pseudomonas fluorescens within the hydrodynamics boundary layers of surface microenvironments. Micro. Ecol. 14, 1–14.

Lyubchenko, Y.L., Oden, P.I., Lampner, D., Lindsay, S.M., Dunker, K.A., 1993. Atomic force microscopy of DNA and bacteriophage in air, water and propanol: the role of adhesion forces. Nucleic Acids Res. 21, 1117–1123.

Manning, P.A., 1995. Use of confocal microscopy in studying bacterial adhesion and invasion. In: Doyle, R.J., Ofek, I. (Eds.), Methods in Enzymology, Vol. 253, Academic Press, California, pp. 159–166.

Ohashi, A., Harada, H., 1996. A novel concept for evaluation of biofilm adhesion strength by applying tensile force and shear force. Wat. Sci. Tech. 34, 201–211.

Oshima, H., Kondo, T., 1991. On the electrophoretic mobility of biological cells. Biophys. Chem. 39, 191–198.

Pembrey, R.S., Marshall, K.C., Schneider, R.P., 1999. Cell surface analysis techniques: what do cell preparation protocols do to cell surface properties. Appl. Environ. Microbiol. 65, 2877–2894.

Radmacher, M., Fritz, M., Hansma, H.G., Hansma, P.K., 1994. Direct observation of enzyme activity with the atomic force microscope. Science 265, 1577–1579.

Razatos, A., Ong, Y.-L., Sharma, M.M., Georgiou, G., 1998. Molecular determinants of bacterial adhesion monitored by atomic force microscopy. Proc. Natl. Acad. Sci. USA. 95, 11059–11064.

Rotsch, C., Radmacher, M., 1997. Mapping local electrostactic forces with the atomic force microscope. Langmuir 13, 2825–2832.

Rutter, P.R., Vincent, B., 1988. Attachment mechanisms in the surface growth of microorganism. In: Bazin, M.J., Prosser, J.I. (Eds.), Physiological Models in Microbiology, CRC Press, Boca Raton, Florida, pp. 87–107.

Teiko, S.S., Wakako, W., Junji, M., 1994. Imaging of cells with atomic force microscopy operated at a ''tapping mode''. J. Vac. Sci. Technol. B 12, 1530–1534.

Van der Werf, K.O., Putman, C.A.J., de Grooth, B.G., Greve, J., 1994. Adhesion force imaging in air and liquid by adhesion mode atomic force microscopy. Appl. Phys. Lett. 65, 1195–1197.

Vandevevere, P., Kirchman, D.L., 1993. Attachment stimulates exopolysaccharide synthesis by a bacterium. Appl. Environ. Microbiol. 59, 3280–3286.

Videla, H.A., 1996. In: Manual of Biocorrosion, Lewis Publishers, Boca Raton, FL, pp. 252.

Xu, L.-C., Fang, H.H.P., Chan, K.-Y., 1999. Atomic force microscopy study of microbiologically influenced corrosion of mild steel. J. Electrochem. Soc. (in press).